Prospects of heavy dark Z_D at multi-TeV muon colliders

Prasenjit Sanyal

CQUeST, Sogang University

Based on Phys.Rev.D 112 (2025) 9, 095010

"Probing a Heavy Dark Z Boson at Multi-TeV Muon Colliders: Leveraging the Optimized Recoil Mass Technique"

Kingman Cheung, Jinheung Kim, Soojin Lee, **Prasenjit Sanyal**, Jeonghyeon Song

Outline

1. Why a new dark $U(1)$ gauge boson? – Commonly referred to as a dark photon A' or dark gauge boson Z_D.

2. Existing constraints and projected sensitivities from future experiments in the Z_D parameter space.

3. Motivations for muon colliders (MuC) as future collider experiment.

4. Search for heavy (TeV scale) Z_D at MuC via annihilation channel $\mu^+\mu^- \to Z_D\gamma$.

Why a new dark $U(1)_D$ gauge boson Z_D?

- Dark matter (DM) particles may interact with each other through a new dark force that is similar to the electromagnetic force felt by ordinary matter.

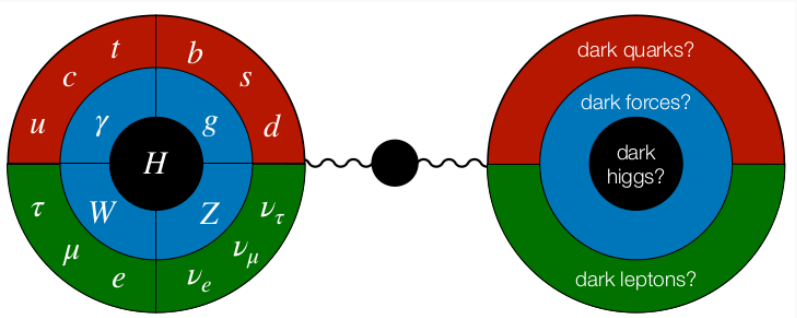

A schematic representation of the dark-sector paradigm

- The dark gauge boson Z_D that mediates this force can obtain a small coupling to the electromagnetic current due to kinetic mixing between the SM hypercharge and $U(1)_D$ field strength tensors via the operator

$$\mathcal{L} \supset \frac{\varepsilon}{2\cos\theta_W} F'_{\mu\nu} B^{\mu\nu}, \qquad \varepsilon \text{ is the kinetic mixing parameter}$$

- The dark Z_D obtains a mass m_{Z_D} via a dark Higgs or Stueckelberg mechanism. The minimal dark Z_D model has only three unknown parameters: m_{Z_D}, ε and Z_D to DM branching ratio (1 if kinematically allowed, 0 if forbidden).

(A) DM (χ) is heavier than Z_D (secluded DM): The DM *freeze-out* is obtained by annihilations to pairs of on-shell Z_D ($\chi\chi \to Z_D Z_D$) followed by Z_D decay to SM particles.

- In this scenario the decay of Z_D is restricted to the visible (SM) sector only.

(B) DM (χ) is lighter than Z_D: The DM annihilation is via $\chi\chi \to Z_D^* \to f\bar{f}$

$$\langle \sigma v \rangle \propto \frac{\varepsilon^2 \alpha_D m_\chi^2}{m_{Z_D}^4} \equiv \frac{y}{m_\chi^2}$$

provides thermal target $-$ large ε and small m_{Z_D}.

- In this scenario, for $m_{Z_D} > 2m_\chi$, $Z_D \to \chi\chi$ decay is nearly 100%.

Production of Z_D in accelerators

1. Bremsstrahlung: $e^- Z \to e^- Z Z_D$ and $pZ \to pZZ_D$ where an incident electron or proton radiates Z_D during an interaction with a fixed nuclear target of charge Z.

2. Annihilation: $e^+e^- \to Z_D\gamma$ at an e^+e^- collider.

3. Drell–Yan: $q\bar{q} \to Z_D$, where a quark and antiquark annihilate into a Z_D, which could occur at a hadron collider or when a proton beam is incident on a fixed nuclear target.

4. Meson decays: $\pi_0 \to Z_D\gamma$ or $\eta \to Z_D\gamma$ for $m_{Z_D} < m_{\pi_0,\eta}$ at any experiment where mesons are produced at high rates.

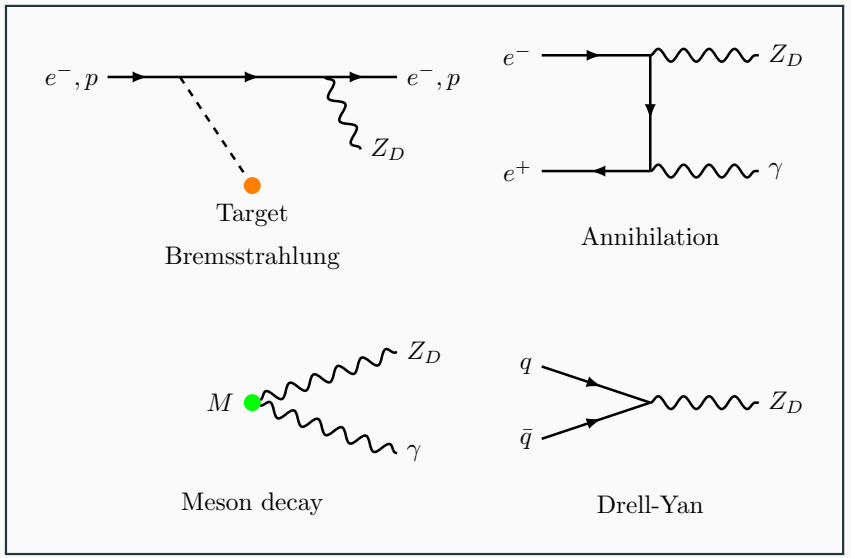

Production of Z_D: Bremsstrahlung, Annihilation, Drell-Yan and Meson decay.

Decays and search strategies

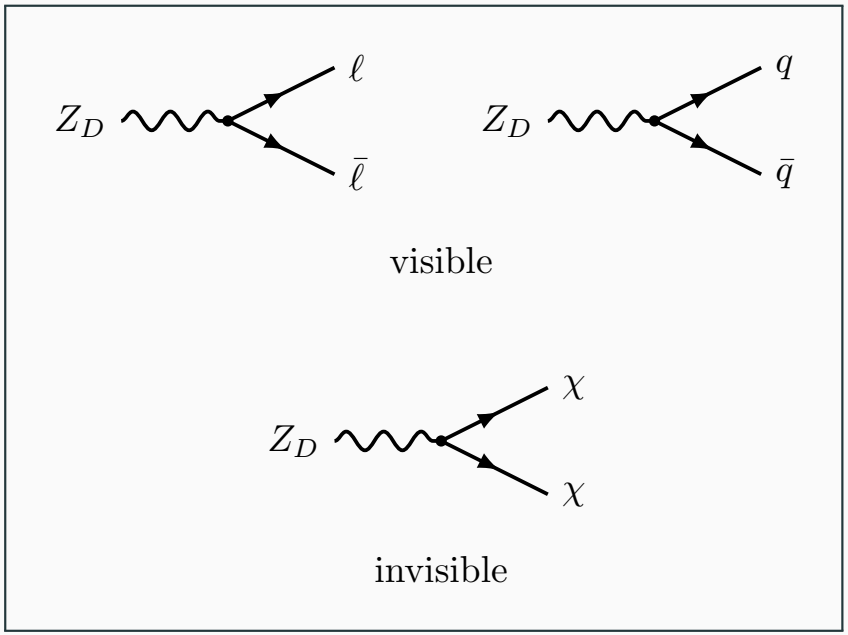

Visible (SM fermions) and invisible (DM) decay modes of Z_D.

Visible decay:

1. The visible decay modes can be prompt if $\varepsilon \gtrsim 10^{-3} \times 10\text{MeV}/m_{Z_D}$.

2. Non-prompt or displace decay for smaller ε and m_{Z_D}. $\tau_{Z_D} \propto (\varepsilon^2 m_{Z_D})^{-1}$.

Invisible decay:

1. if $m_{Z_D} > 2m_\chi$, Z_D decays to DM by 100%

2. Seach strategies look for events with an imbalance of energy and momentum.

3. Search for the rare interactions of the DM particles in a detector placed downstream of the Z_D decay point.

Current Constraints and projected sensitivities

Visibly decaying Z_D:

1. Current constraints from electron beam dumps (red), proton beam dumps (light blue), e^+e^- colliders (green), pp collisions (dark blue), meson decays (purple), and electron-on-fixed-target experiments (yellow).

2. Proposed future sensitivities with the same color schemes.

"Searches for dark photons at accelerators", arXiv: 2104.10280

Existing limits

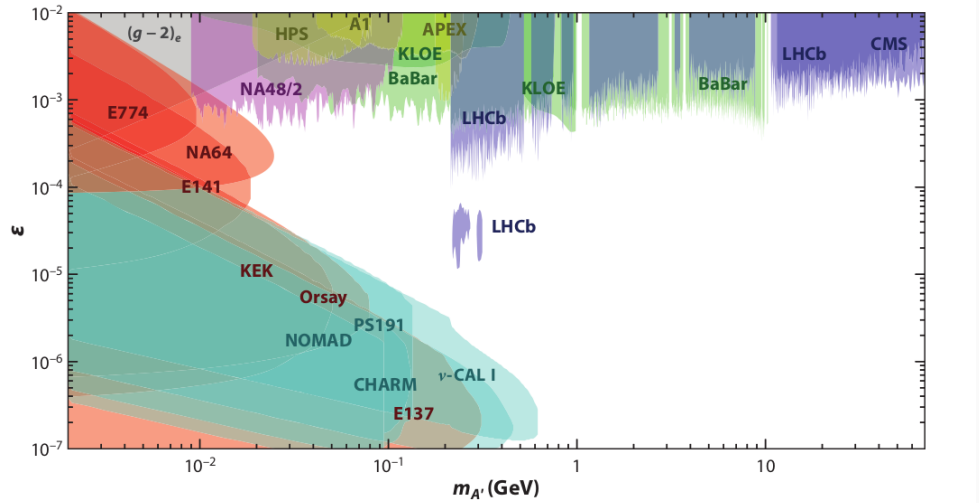

Projected sensitivities

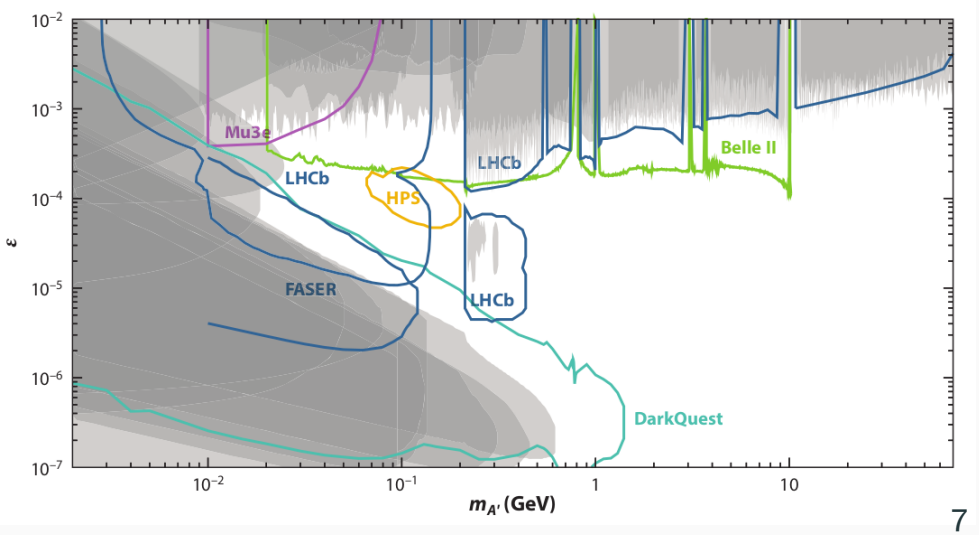

Existing limits and Projected sensitivities

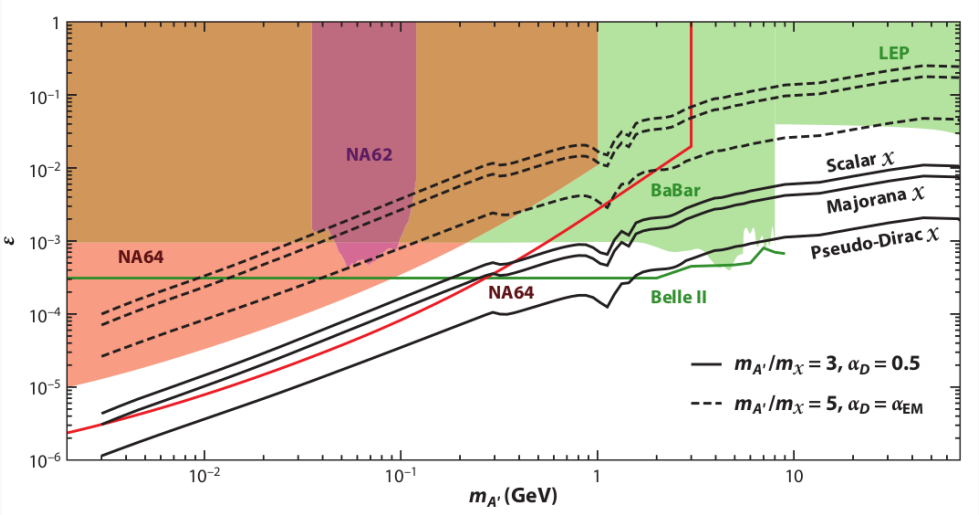

Existing limits and Projected sensitivities

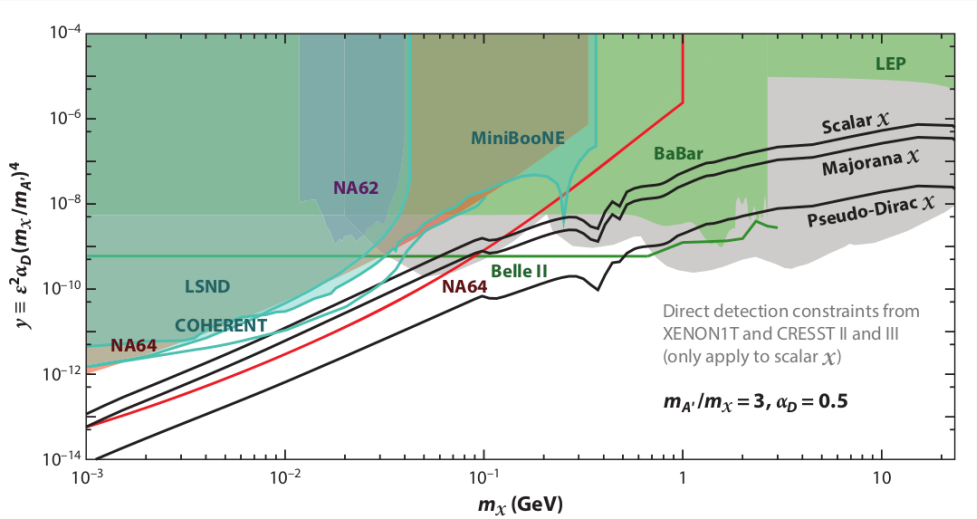

Invisibly decaying Z_D:

1. Constraints and proposed sensitivity from e^+e^- colliders (green), electron beam dump (red) and meson decay (purple).

2. Constraints on the invisible $Z_D \to \chi\chi$ scenario in the (m_χ, y) plane. Searches for dark Z_D produced in proton beam dumps with the subsequent scattering of χ particles in a detector placed downstream of the Z_D decay point are shown using light blue.

"Searches for dark photons at accelerators", arXiv: 2104.10280

Why Muon Colliders (MuC)?

Advantages:

1. Future muon colliders (MuC) could be ideal for achieving both high energy and high luminosity.
2. Reduced synchrotron radiation $\frac{1}{R}(\frac{E}{m})^4$, compared to e^+e^- colliders.
3. A few TeV MuC is as efficicient as a 100 TeV hadron collider.
4. Much lower background compared to hadron colliders.

Disadvantages:

1. Muons are unstable with a lifetime of 2μs.
2. Difficult to produce low emittance muon beams.
3. Beam induced backgrounds or BIBs.

MuC is at the conceptual stage...

Probing TeV scale Z_D at MuC

- For a heavy Z_D with a mass above 1 TeV, constraints become weaker.

- Existing studies have focused on pp colliders via the Drell-Yan process $pp \to Z_D \to \ell\ell$.

- At **HL-LHC** (14 TeV & 3 ab^{-1}), the projected sensitivity reaches $\varepsilon \sim 10^{-2}$ and 10^{-1} for $m_{Z_D} \sim 1$ TeV and 2.5 TeV respectively.

- At **FCC-hh** (100 TeV & 3 ab^{-1}), can improve to $\varepsilon \sim 4 \times 10^{-3}$ and 3×10^{-2} for $m_{Z_D} \sim 1$ TeV and 2.5 TeV respectively.

- At MuC $2 \to 2$ and $2 \to 3$ annihilation channels:

  1. $\mu^+\mu^- \to Z_D\gamma$
  2. $\mu^+\mu^- \to Z_D\nu\nu$
  3. $\mu^+\mu^- \to Z_D\mu^+\mu^-$

  with $p_T^{\gamma,\mu} > 10$ GeV, $|\eta| < 2.5$ and $E_{miss}^T > 10$ GeV.

The $2 \to 2$ annihilation $\mu^+\mu^- \to Z_D\gamma$ appears most promising

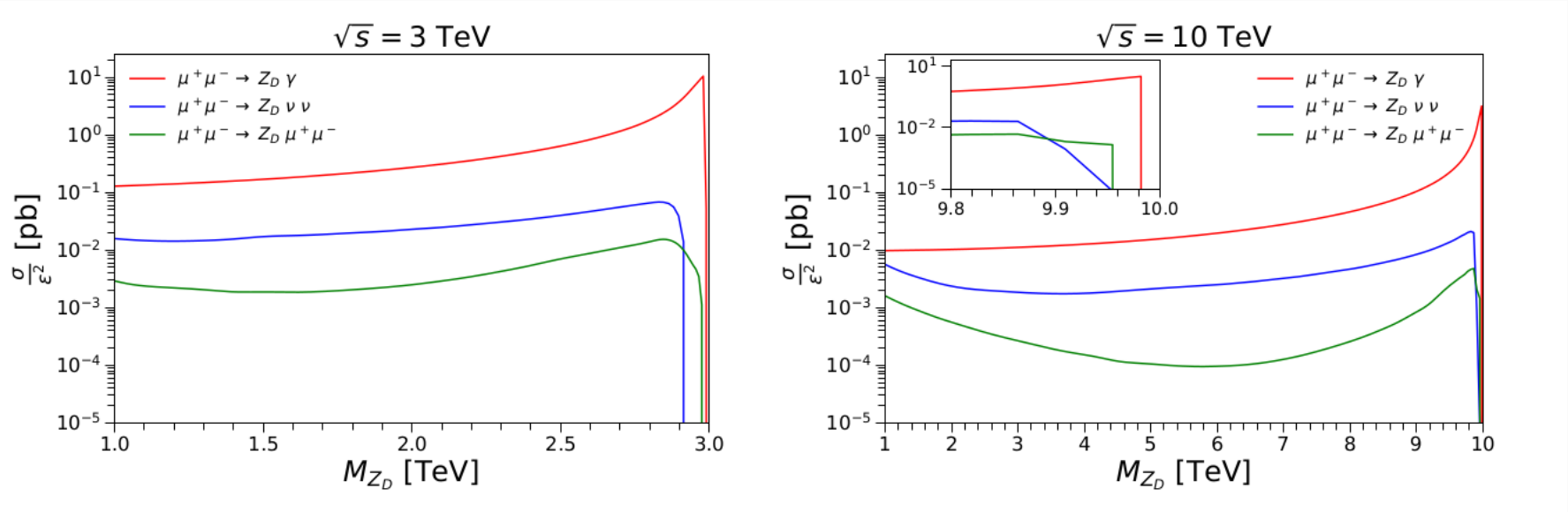

Kingman Cheung, Jinheung Kim, Soojin Lee, **Prasenjit Sanyal**, Jeonghyeon Song, Phys.Rev.D 112 (2025) 9, 095010

Z_D decay modes

- Two key decay modes at the MuC: $Z_D \to j\,j\,X$ (inclusive dijet) and $Z_D \to e^+e^-$.
- The inclusive dijet mode combines multiple hadronic final states ($q\bar{q}$, $t\bar{t}$, $\tau\bar{\tau}$, and WW) maximizes the signal yield.
- e^+e^- mode provides a cleaner final state compared to the $\mu^+\mu^-$ decay mode.

- The signal is categorized into:
  1. $\mu^+\mu^- \to Z_D\gamma, \quad Z_D \to j\,j\,X$
  2. $\mu^+\mu^- \to Z_D\gamma, \quad Z_D \to e^+e^-$

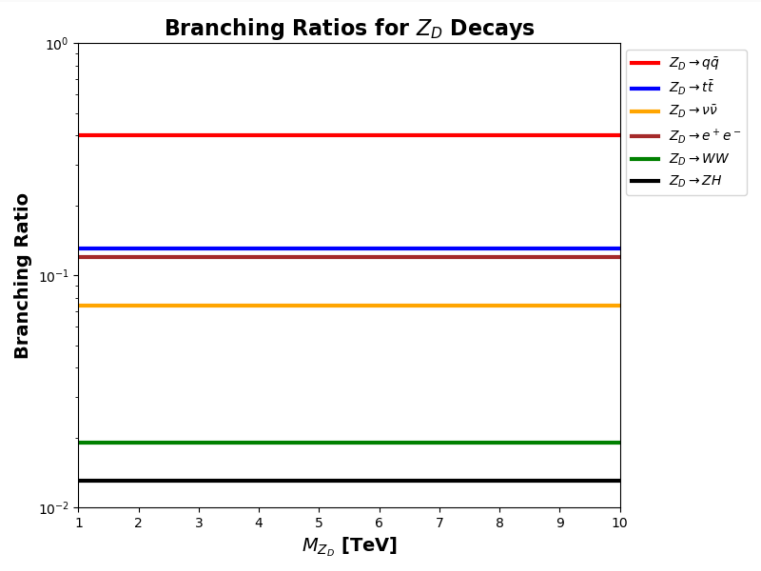

Photon recoil mass

- For the process

$$\mu^+(p_1) + \mu^-(p_2) \to Z_D(p_{Z_D}) + \gamma(p_\gamma)$$

The recoil mass of the photon is defined as

$$\begin{aligned} m^2_{\text{recoil}} &= (p_1 + p_2 - p_\gamma)^2 \equiv m^2_{Z_D} \\ &= s - 2\sqrt{s}E_\gamma \end{aligned}$$

The recoil mass measures the mass of Z_D independent of its decay mode.

- At the detector, the photon recoil mass (m_{recoil}) and e^+e^- invariant mass (m_{ee}) distributions depend strongly on the energy resolutions of γ, e^-, e^+.

- Typically the energy resolution is expressed as:

$$\left(\frac{\Delta E}{E}\right)^2 = \left(\frac{a(\eta)}{\sqrt{E}}\right)^2 + \left(\frac{b(\eta)}{E}\right)^2 + c(\eta)^2$$

A. $m_{Z_D} \to \sqrt{s}$, $E_\gamma \to 0 \implies$ sharp photon m_{recoil} distribution.

B. $m_{Z_D} \ll \sqrt{s}$, $E_\gamma \gg 0 \implies$ broad photon m_{recoil} distribution.

C. m_{ee} distribution exhibits the opposite behavior.

Photon recoil mass m_{recoil} (blue) and the e^+e^- invariant mass m_{ee} (orange) for $\mu^+\mu^- \to Z_D(\to e^+e^-)\gamma$ at $\sqrt{s} = 3$ TeV and 10 TeV MuC.

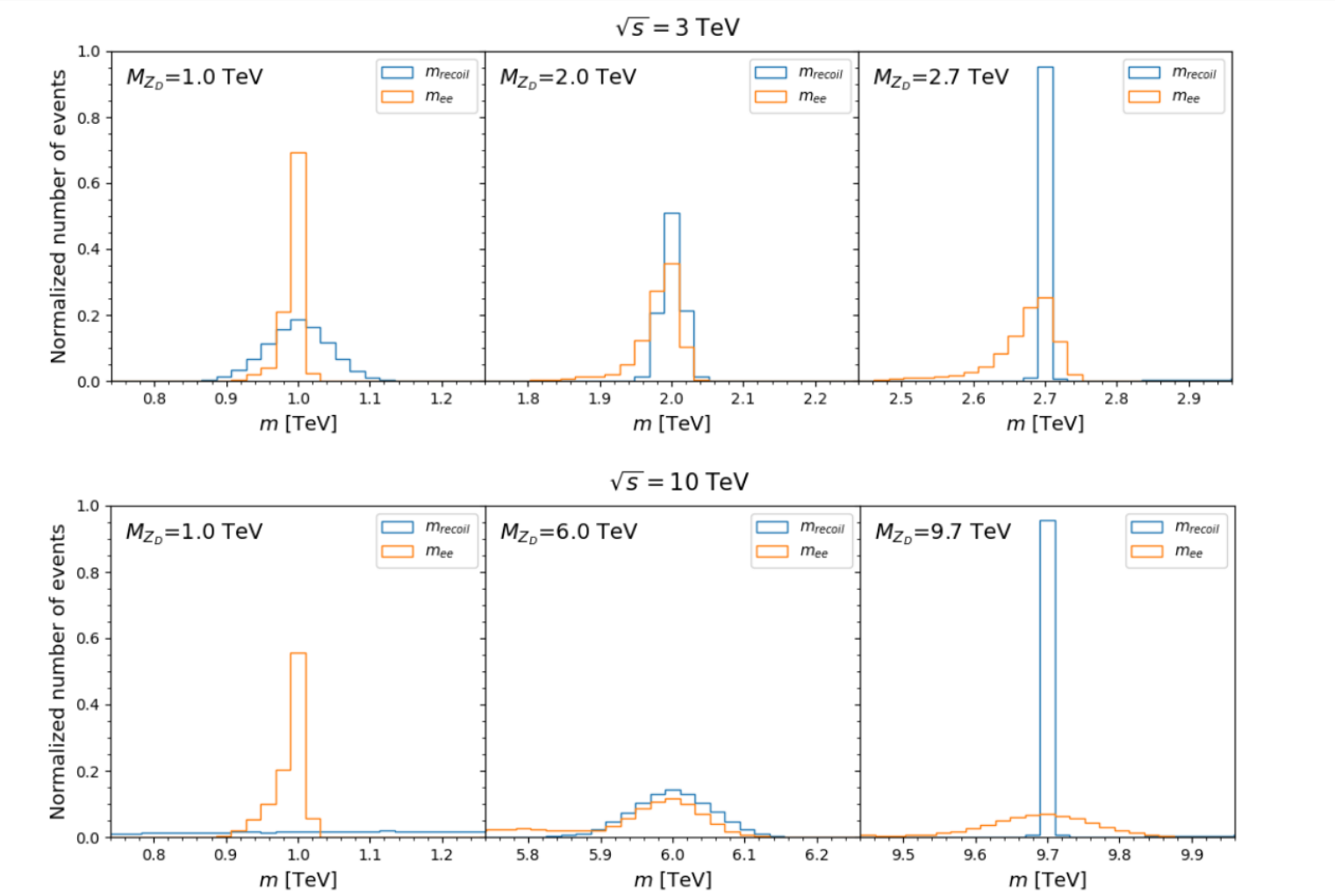

Kingman Cheung, Jinheung Kim, Soojin Lee, **Prasenjit Sanyal**, Jeonghyeon Song, Phys.Rev.D 112 (2025) 9, 095010

The m_{recoil} and m_{ee} distributions were then fitted with Gausian distributions to obtain the widths Δm_{recoil} and Δm_{ee} as the standard deviations of the Gausian fits.

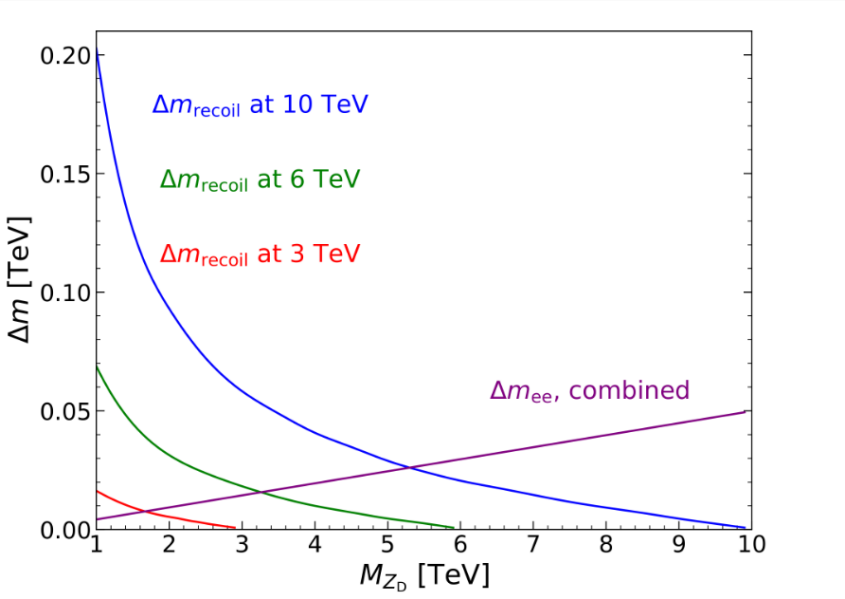

Kingman Cheung, Jinheung Kim, Soojin Lee, **Prasenjit Sanyal**, Jeonghyeon Song, Phys.Rev.D 112 (2025) 9, 095010

Key characteristics:

1. Δm_{recoil} decreases with increasing m_{Z_D}.
2. For a fixed m_{Z_D}, Δm_{recoil} increases with $\sqrt{s}$.
3. m_{ee} increases with m_{Z_D}.
4. Δm_{recoil} and m_{ee} intersects around $m_{Z_D} \simeq \sqrt{s}/2$.

Signal and background

- We consider scattering processes within $|\eta| < 2.5$; $p_T^{\gamma} > 20$ GeV; $p_T^{j_1,e_1} > 100$ GeV and $p_T^{j_2,e_2} > 20$ GeV for the leading and subleading jets or electrons.
- To categorize the two channels we require:

$$jjX \begin{cases} N_j \geq 2 & N_\gamma \geq 1 \\ N_{e,\mu} = 0 & \text{lepton veto with } p_T > 20 \text{ GeV} \end{cases}$$

and

$$e^+e^-\gamma \begin{cases} N_e \geq 2 & N_\gamma \geq 1 \\ N_j = 0 & \text{jet veto with } p_T > 20 \text{ GeV} \end{cases}$$

- Two different mass window cuts:
  1. $m_{\text{recoil}} = m_{Z_D} \pm 2\Delta m_{\text{recoil}}$
  2. $m_{ee} = m_{Z_D} \pm 2\Delta m_{ee}$
- Dominant backgrounds:
  1. $\mu^+\mu^- \to jj\gamma$
  2. $\mu^+\mu^- \to e^+e^-\gamma$

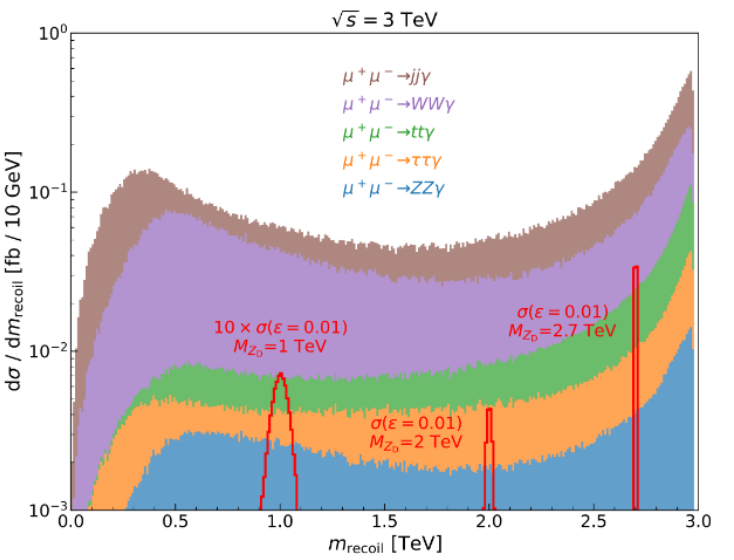

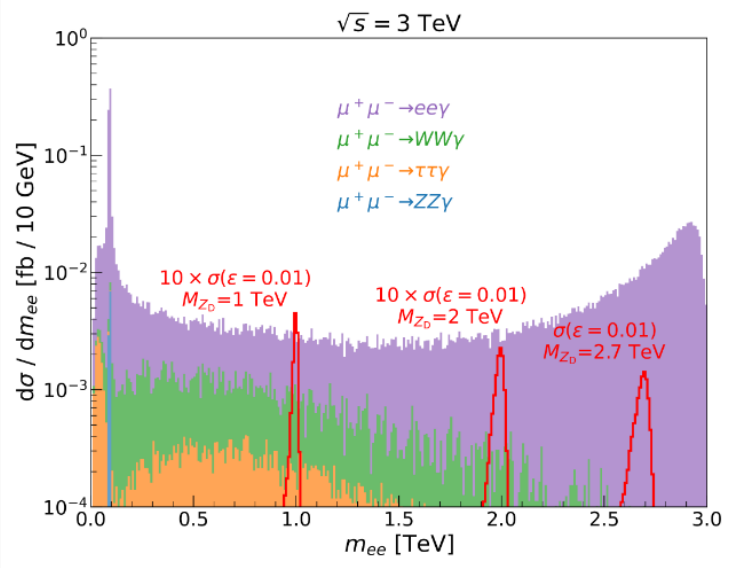

2σ contours for detecting Z_D through the processes: $\mu^+\mu^- \to Z_D(\to jjX)\gamma$ (left) and $\mu^+\mu^- \to Z_D(\to e^+e^-)\gamma$ (right).

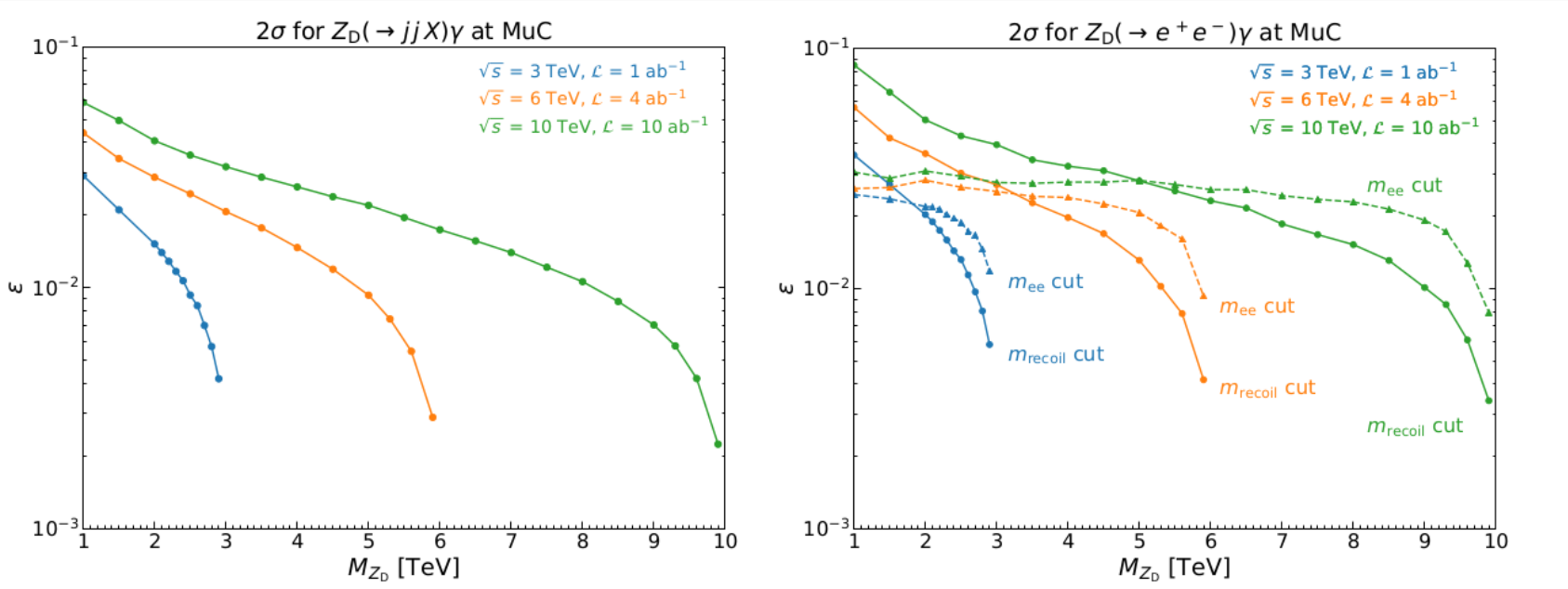

Phys.Rev.D 112 (2025) 9, 095010

- jjX mode, m_{recoil} selection cut can be used only.
- $ee\gamma$ mode, both the m_{recoil} and m_{ee} selection cuts can be used.
- For the $ee\gamma$ mode, the optimum choice is: m_{recoil} cut for $m_{Z_D} > \sqrt{s}/2$ and m_{ee} cut for $m_{Z_D} < \sqrt{s}/2$.
- Statistical significance:

$$\mathcal{S} = \sqrt{2\left[(n_s + n_b)\ln\left(\frac{n_s + n_b}{n_b}\right) - n_s\right]}, \quad \mathcal{S}_{\text{tot}} = \sqrt{\mathcal{S}^2_{jjX} + \mathcal{S}^2_{ee\gamma}}$$

Results

2σ (solid lines) and 5σ (dashed lines) contours for detecting Z_D, combining the processes: $\mu^+\mu^- \to Z_D(\to jjX)\gamma$ and $\mu^+\mu^- \to Z_D(\to e^+e^-)\gamma$.

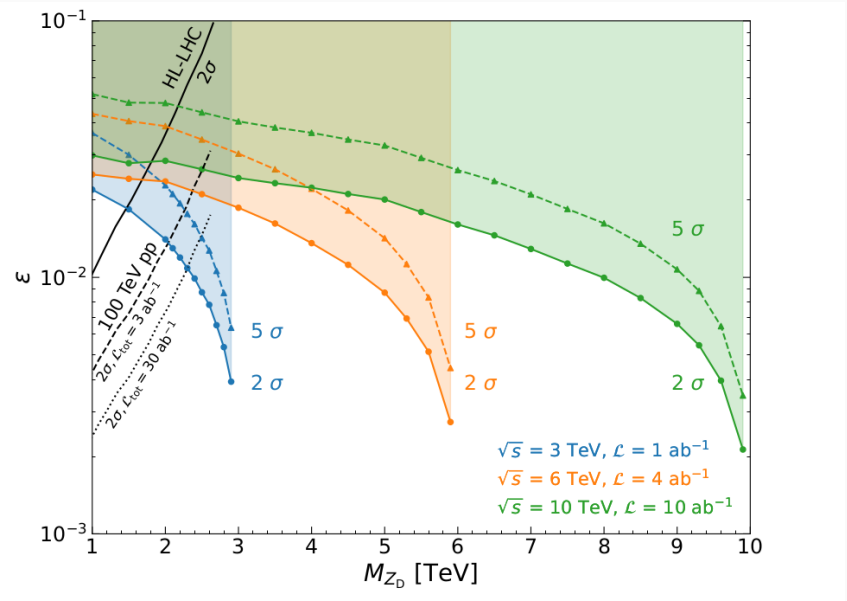

Phys.Rev.D 112 (2025) 9, 095010

- The $ee\gamma$ mode outperforms at low m_{Z_D} and jjX mode outperforms at high m_{Z_D}. The improvement of combining both the channels is betweed $3\% - 10\%$.
- 2σ contours of HL-LHC and FCC-hh shows that MuC clearly outperforms at hingher m_{Z_D}.

Conclusions

- Brief overview of dark Z_D boson. Current constraints and future sensitivities on the $m_{Z_D} - \varepsilon$ space.
- Brief discussion on muon colliders as future collider experiment.
- Search for heavy Z_D at MuC via annihilation channel $\mu^+\mu^- \to Z_D\gamma$.
- Optimised the photon recoil mass and the electron-positron invariant mass cuts to achieve the best sensitivity.

Background cross sections in units of fb			
Processes	$\sqrt{s} = 3$ TeV	$\sqrt{s} = 6$ TeV	$\sqrt{s} = 10$ TeV
$\mu^+\mu^- \to jj\gamma$	5.01×10	1.40×10	5.44
$\mu^+\mu^- \to e^+e^-\gamma$	9.31	2.75	1.10
$\mu^+\mu^- \to W^+W^-\gamma$	2.55×10	1.01×10	4.86
$\mu^+\mu^- \to \tau^+\tau^-\gamma$	5.37	1.63	6.67×10^{-1}
$\mu^+\mu^- \to t\bar{t}\gamma$	3.24	1.07	4.58×10^{-1}
$\mu^+\mu^- \to ZZ\gamma$	2.25	8.30×10^{-1}	3.82×10^{-1}

Background cross sections

Cut-flow of cross sections (fb) for $\mu^+\mu^- \to Z_{\rm D}(\to jjX)\gamma$ at a 3 TeV MuC with $\mathcal{L}_{\rm tot} = 1$ ab^{-1}						
$M_{Z_{\rm D}} = 1$ TeV & $\varepsilon = 0.01$						
Cut	$Z_{\rm D}(\to jj)\gamma$	$jj\gamma$	$W^+W^-\gamma$	$\tau^+\tau^-\gamma$	$t\bar{t}\gamma$	$\mathcal{S}_{1\,\text{ab}^{-1}}$
Basic	7.69×10^{-3}	1.42×10	1.15×10	1.08	1.86	4.47×10^{-2}
$\lvert m_{j_1} - m_W\rvert > 20$ GeV	6.34×10^{-3}	1.20×10	3.75	1.08	1.51	4.64×10^{-2}
$\lvert m_{\rm recoil} - M_{Z_{\rm D}}\rvert < 2\Delta m_{\rm recoil}$	3.47×10^{-3}	9.37×10^{-2}	8.47×10^{-2}	1.01×10^{-2}	1.29×10^{-2}	2.40×10^{-1}
$M_{Z_{\rm D}} = 2.7$ TeV & $\varepsilon = 0.01$						
$\lvert m_{\rm recoil} - M_{Z_{\rm D}}\rvert < 2\Delta m_{\rm recoil}$	3.12×10^{-2}	3.32×10^{-2}	6.22×10^{-3}	4.20×10^{-3}	7.72×10^{-3}	3.96

Table II: Cut-flow of cross sections in units of fb for the signal $\mu^+\mu^- \to Z_{\rm D}(\to jjX)\gamma$ with $\varepsilon = 0.01$ and $M_{Z_{\rm D}} = 1$ TeV and 2.7 TeV at the 3 TeV MuC. The significance $\mathcal{S}_{1\,\text{ab}^{-1}}$ is calculated assuming an integrated luminosity of 1 ab^{-1}. Note that $\Delta m_{\rm recoil}$ and Δm_{ee} values depend on $M_{Z_{\rm D}}$.

Cut-flow of cross sections [fb] for $\mu^+\mu^- \to Z_{\rm D}(\to jjX)\gamma$ at a 10 TeV MuC with $\mathcal{L}_{\rm tot} = 10\ {\rm ab}^{-1}$						
$M_{Z_{\rm D}} = 1$ TeV & $\varepsilon = 0.01$						
Cut	$Z_{\rm D}(\to jj)\gamma$	$jj\gamma$	$W^+W^-\gamma$	$\tau^+\tau^-\gamma$	$t\bar{t}\gamma$	$\mathcal{S}_{10\,{\rm ab}^{-1}}$
Basic	5.09×10^{-4}	1.21	1.86	1.37×10^{-1}	2.91×10^{-1}	2.69×10^{-2}
$\lvert m_{j_1} - m_W\rvert > 20$ GeV	4.02×10^{-4}	9.25×10^{-1}	5.14×10^{-1}	1.33×10^{-1}	2.78×10^{-1}	2.93×10^{-2}
$\lvert m_{\rm recoil} - M_{Z_{\rm D}}\rvert < 2\Delta m_{\rm recoil}$	2.28×10^{-4}	4.55×10^{-2}	9.00×10^{-2}	4.49×10^{-3}	9.23×10^{-3}	5.85×10^{-2}
$M_{Z_{\rm D}} = 9.7$ TeV & $\varepsilon = 0.01$						
$\lvert m_{\rm recoil} - M_{Z_{\rm D}}\rvert < 2\Delta m_{\rm recoil}$	1.18×10^{-2}	3.18×10^{-3}	9.43×10^{-4}	3.95×10^{-4}	1.20×10^{-3}	12.4

Table III: Cut-flow of the cross sections in units of fb for the signal $\mu^+\mu^- \to Z_{\rm D}(\to jjX)\gamma$ with $\varepsilon = 0.01$ and $M_{Z_{\rm D}} = 1\ {\rm TeV}, 9.7\ {\rm TeV}$ at the 10 TeV MuC. The significance $\mathcal{S}_{10\,{\rm ab}^{-1}}$ is calculated considering an integrated luminosity of 10 ${\rm ab}^{-1}$. Note that $\Delta m_{\rm recoil}$ and Δm_{ee} values depend on $M_{Z_{\rm D}}$.

Final selection results for $\mu^+\mu^- \to Z_{\rm D}(\to e^+e^-)\gamma$ at a 3 TeV MuC with $\mathcal{L}_{\rm tot} = 1\ {\rm ab}^{-1}$						
	$m_{\rm recoil}$ cut		m_{ee} cut		combined	
	$\sigma_{\rm sig}$ [fb]	$\mathcal{S}_{1\,{\rm ab}^{-1}}$	$\sigma_{\rm sig}$ [fb]	$\mathcal{S}_{1\,{\rm ab}^{-1}}$	$\sigma_{\rm sig}$ [fb]	$\mathcal{S}_{1\,{\rm ab}^{-1}}$
$M_{Z_{\rm D}} = 1$ TeV	6.01×10^{-4}	1.69×10^{-1}	6.88×10^{-4}	3.75×10^{-1}	3.79×10^{-4}	3.04×10^{-1}
$M_{Z_{\rm D}} = 2.7$ TeV	5.91×10^{-3}	2.12	5.71×10^{-3}	7.37×10^{-1}	3.23×10^{-3}	1.61

Table V: Signal cross sections and significances for $\mu^+\mu^- \to Z_D(\to e^+e^-)\gamma$ at a 3 TeV MuC with $\mathcal{L}_{\rm tot} = 1\ {\rm ab}^{-1}$, shown for $M_{Z_{\rm D}} = 1$ TeV and $M_{Z_{\rm D}} = 2.7$ TeV. We fixed $\varepsilon = 0.01$. Results are presented after basic selection, $E_{ee\gamma} > 0.9\sqrt{s}$ cut, and three final selection criteria: (1) $m_{\rm recoil}$ cut, (2) m_{ee} cut, and (3) combined cut applying both conditions.